Deposition of Gold Films and Nanostructures from Supercritical Carbon Dioxide

Albertina Cabañas,† David P. Long,† and James J. Watkins*

Department of Chemical Engineering, University of Massachusetts, Amherst, Massachusetts 01003

Received August 8, 2003. Revised Manuscript Received December 1, 2003

High-purity gold films were deposited onto metal, ceramic, and polymer substrates by the H_2-assisted reduction of dimethyl(acetylacetonate)gold(III) in supercritical CO_2 at temperatures between 60 and 125 °C. At 125 °C and 150 bar, Au deposition proceeded readily on all surfaces studied, including SiO_2 and TiN films. By contrast, at 60 °C and 138 bar, deposition was highly selective for metal substrates including nickel and palladium films over nongrowth surfaces such as polymers or the native oxide of silicon. Low-temperature deposition on nongrowth surfaces was possible by seeding the substrate with Pt, Pd, or Ni clusters or films. In all cases, Au films deposited from CO_2 were conformal. Excellent step coverage on Si wafers was achieved in features ranging from 0.1 to 1.0 μm wide by 1.0 μm deep. Continuous arrays of gold posts were prepared using etched Si wafers backfilled with SiO_2 as templates. Following gold deposition at 125 °C, the arrays were released from the template by selective etching of the SiO_2 layer with HF. The features of the substrate were accurately replicated in the gold film. Postdeposition analysis of the CO_2 effluent stream by ^{1}H NMR revealed that ethane and 2,4-pentanedione were the only major ligand products of precursor reduction.

Introduction

Gold films and deposits are used extensively in device structures. In microelectronics, gold's low electrical resistivity (2.35 μohm cm/20 °C) and resistance to corrosion and chemical attack is exploited in contacts, gate arrays, and other features.[1−5] Moreover gold surfaces modified with thiol-based self-assembled monolayers are being evaluated for a broad range of applications including biosensors in DNA chips[6] and detection arrays for airborne contaminants.[7] In many applications, conformal coverage on complex surface topographies or low-temperature deposition is required. In principle, the former could be achieved via chemical vapor deposition (CVD). There are a number of gold(I) and gold(III) compounds with sufficient vapor pressure and efficient mechanisms for thermal reduction that have been investigated for use in CVD, including dialkyl gold(III) β-diketonates, trialkylgold(III) compounds, and monoalkylgold(I) phosphines.[8−16] However, deposition temperatures between 200 and 300 °C are typically required for high-purity films, and mass-transfer limitations often preclude uniform deposition in demanding device features.[17,18] Low-temperature deposition can be achieved via electroless or electrolytic plating,[19] however, the use of plating baths containing potassium gold cyanide and reducing agents such as hypophosphite, hydrazine, or formaldehyde present environmental challenges. Moreover, electrolytic plating requires continuous seed layers or conductive substrates.

We recently reported an alternative technique called chemical fluid deposition (CFD) that can be used to deposit metals from supercritical fluids (SCF) onto planar surfaces and patterned substrates for device fabrication. CFD involves the chemical reduction of organometallic compounds in SCFs to yield high-purity deposits.[20] The reaction is initiated upon the addition

* To whom correspondence should be addressed. E-mail: watkins@ecs.umass.edu.

† These individuals contributed equally to the work.

(1) Holliday, R.; Goodman, P. *IEE Rev.* **2002**, *48*, 15−19.
(2) Oren, M.; Masum Chounury, A. N. M. *J. Electrochem. Soc.* **1987**, *134*, 750−752.
(3) Baum, T. H.; Comita, P. B.; Kodas, T. T. *SPIE Symp. Lasers Microelec. Manufac.* **1991**, *122*, 1598.
(4) Wassick, T. A. In *Proceedings of the SPIE Symposium on Lasers in Microelectronic Manufacturing*; vol. 1598; International Society for Optical Engineering: Bellingham, WA, 1991; p 141.
(5) Chiu, S. L.; Acosta, R. E. *J. Vac. Sci. Technol. B* **1990**, *8*, 1589.
(6) Pirrung, M. C. *Angew. Chem., Int. Ed.* **2002**, *41*, 1276−1289.
(7) Shah, R. R.; Abbott, N. L. *Science* **2001**, *293*, 1296−1299.
(8) Kodas, T. T.; Hampden-Smith, M. J. *The Chemistry of Metal CVD*; VCH: Weinheim, 1994.
(9) Hampden-Smith, M. J.; Kodas, T. T. *Chem. Vap. Deposition* **1995**, *1*, 8−23.
(10) Hampden-Smith, M. J.; Kodas, T. T. *Chem. Vap. Deposition* **1995**, *1*, 39−48.
(11) Puddephatt, R. J. *Polyhedron* **1994**, *13*, 1233−1243.
(12) Puddephatt, R. J. In *Topics in Inorganic Chemistry and General Chemistry*; Clark, R. J. H., Ed.; Elsevier: Amsterdam, 1978.
(13) Larson, C. E.; Baum, T. H.; Jackson, R. L. *J. Electrochem. Soc.* **1987**, *134*, 226.
(14) Banaszak, M. M.; Seidler, P. F.; Kowalczyk, S. P.; McFreely, F. R. *Inorg. Chem.* **1994**, *33*, 510−517.
(15) Allen, D. W.; Haigh, J. *Appl. Organomet. Chem.* **1995**, *9*, 83−88.
(16) Seidler, P. F.; Kowalczyk, S. P.; Banaszak, M. M.; Yurkas, J. J.; Norcott, M. H.; McFreely, F. R. *Mater. Res. Soc. Symp. Proc.* **1993**, *282*, 359.
(17) Kodas, T. T.; Baum, T. H.; Comita, P. B. *J. Appl. Phys.* **1987**, *62*, 281−286.
(18) Holloway, K.; Zuhoski, S. P.; Reynolds, S.; Matuszewski, C. *Mater. Res. Soc. Symp. Proc.* **1991**, *204*, 409.
(19) Lawrence, D. J. e. *Electroplating Engineering Handbook*; 4th ed.; Van Nostrand Reinhold: New York, 1984.

10.1021/cm034739u CCC: $27.50
Published on Web 00/00/0000 PAGE EST: 5.5

of H_2 or another reducing agent. Supercritical CO_2 ($scCO_2$) is used in most of the deposition experiments, although other fluids can be used.[21] The advantages of CFD over conventional deposition techniques are a consequence of the unique properties of SCFs, which lie intermediate to those of liquids and gases.[22] Because liquidlike densities can be achieved at modest pressures, many organometallic compounds are soluble in $scCO_2$. Although CFD is a solution-based technique, the transport properties of $scCO_2$ (low viscosity and high diffusivity relative to liquids), the absence of surface tension and its miscibility with gaseous reducing agents such as H_2[23] promote infiltration in complex geometry and mitigate mass transfer limitations common to liquid-phase reductions. Moreover, the presence of $scCO_2$ facilitates desorption of ligand decomposition products, which reduces contamination of the metal film. Palladium, platinum, nickel, copper, rhodium, and cobalt films have been successfully deposited using this technique.[21,24−31] In a brief communication we previously reported the deposition of gold films by the H_2 reduction of dimethyl(acetylacetonate)gold(III) [(acac)-$Au(CH_3)_2$] solutions in $scCO_2$ at 60 °C and 138 bar.[26] At this temperature, high-purity films were deposited selectively on metals over glass and polyimide. Despite the low temperature, the films were free of oxygen and carbon contamination as verified by X-ray photoelectron spectroscopy. In this paper we extend these results to a broader range of substrates and to higher temperature (125 °C), where the deposition occurred on all surfaces studied. We also deposited gold onto patterned wafers to demonstrate void-free trench and via filling and took advantage of the exceptional step coverage of CFD to produce nanostructures by using an etched silicon wafer as a sacrificial template. Finally, analysis of the reaction byproduct by NMR spectroscopy provided insight into the deposition mechanism in CO_2.

Experimental Section

Dimethyl(acetylacetonate)gold(III) [(acac)$Au(CH_3)_2$] was purchased from Strem Chemical and used as received in the deposition experiments. For experiments designed for analysis of the reduction products by NMR, [(acac)$Au(CH_3)_2$] was sublimed prior to use (80 °C at 0.2 Torr) yielding long white crystals of precursor. Bis(cyclopentadienyl)nickel(II) [$(Cp)_2Ni$] and (1,5-cyclooctadiene) dimethylplatinum(II) (98%) [(COD)-$Pt(CH_3)_2$] were obtained from Aldrich. $(Cp)_2Ni$ was sublimed prior to use (80 °C at 0.2 Torr) but [COD]$Pt(CH_3)_2$ was used as received. All organometallic precursors were stored under inert atmospheres of nitrogen. [(acac)$Au(CH_3)_2$] and $(Cp)_2Ni$ were stored at 0 °C. 2-Methylallylcyclopentadienylpalladium-(II) [$CpPd(\pi^3\text{-}C_4H_7)$] was prepared as described previously,[25] sublimed prior to each use (60 °C at 0.2 Torr), and stored at 0 °C.

Silicon test wafers with a (100) or (111) orientation were purchased from International Wafer Service. Depositions were carried out directly on the native oxide. Silicon wafers with a 300 Å TiN barrier layer and etched Si test wafers with a SiO_2 back-fill layer were donated by Novellus Systems. Strips of Kapton polyimide of 50-μm thickness were cut into 3 × 0.5 in. pieces, cleaned by immersion in boiling deionized water followed by sonication in anhydrous methanol (VWR) for 1 h, and dried overnight in air at 150 °C. Nickel foil (99.95%) was purchased from Aldrich, cut into strips, and cleaned using a procedure similar to that used for the polyimide. Carbon dioxide (Coleman grade) and hydrogen (ultrahigh-purity grade) were obtained from Merriam-Graves and used as received.

Most supercritical CO_2 deposition experiments were carried out in 17-mL high-pressure stainless steel vessels (High-Pressure Equipment Company). Substrates of known weight and a known mass of (acac)$Au(CH_3)_2$ were loaded into the high-pressure vessels inside a glovebox. The vessels were sealed, placed in a constant-temperature circulating bath (60 °C), and allowed to equilibrate. Then the reaction vessels were charged with CO_2 at pressures up to 138 bar using a high-pressure syringe pump (Isco, Inc. model 500HP) maintained at the same temperature as the circulating bath. At these conditions, (acac)$Au(CH_3)_2$ dissolves appreciably in $scCO_2$.[26] The vessel contents were mechanically mixed and returned to the constant-temperature bath for 30 min to ensure complete dissolution of the precursor. Then a 20−100 molar excess of H_2 was slowly added to the reaction vessels using a small (3.8 mL) high-pressure manifold via pressure drop. After H_2 addition, the reactions were allowed to proceed for a period between 4 and 24 h.

The deposition of Pd and Pt metal seed layers was carried out in the same reactors using the same procedure with an appropriate precursor.[25] Ni seed layers were prepared by co-depositing Pd and Ni from solutions of [$(Cp)_2Ni$] and trace [$CpPd(\pi^3\text{-}C_4H_7)$] in supercritical CO_2 following a procedure previously described.[28] The metal-seeded substrate was then sealed inside another high-pressure vessel and gold was deposited by H_2 reduction of (acac)$Au(CH_3)_2$ solution in CO_2 as previously described.

The experiments conducted at 125 °C were carried out using a ∼100-mL stainless steel high-pressure cold-wall reactor except as noted. The cold-wall reactor is a two-flanged high-pressure vessel with an electrically heated stage.[28] The temperature of the walls and the stage are controlled independently. In these experiments, the walls of the reactor were heated at 60 °C using heating cartridges while the stage was heated resistively to 125 °C. Deposition of gold does not proceed readily on unseeded surfaces at temperatures below 125 °C. By keeping the walls at a temperature lower than the stage, selective deposition onto the heated substrate was achieved. The experiments were conducted in batch mode. The solid precursor and a substrate were loaded into the reactor and the vessel was sealed and purged with N_2. Then the reactor was heated at 60 °C and CO_2 was loaded from a high-pressure syringe pump (Isco, Inc. model 500HP), which was kept at 60 °C, to a pressure of 125 bar. The precursor was allowed to dissolve in CO_2 for 30 min after which a 100× molar excess of H_2 was added from a 70-mL manifold via pressure-drop. Then the pedestal was heated to 125 °C while keeping the walls at 60 °C. The final pressure was ∼150 bar. In each experiment the pedestal was heated for 3−4 h. After the deposition experiments, the reactor contents were vented through an activated carbon bed. In selected cases, the reaction byproducts were vented through a bubbler containing an appropriate solvent upstream of the carbon bed for subsequent analysis. The mass of the deposited film was determined using a precision balance and used to estimate the thickness of the films.

(20) Watkins, J. J.; McCarthy, T. J. Method of Chemically Depositing Material onto a Substrate. U.S. Patent 5,789,027, 1998.
(21) Cabañas, A.; Blackburn, J. M.; Watkins, J. J. *Microelectron. Eng.* **2002**, *64*, 53−61.
(22) McHugh, M. A.; Krukonis, V. J. *Supercritical Fluid Extraction: Principles and Practice*; Butterworth: Boston, 1986.
(23) Tsang, C. Y.; Street, W. B. *Chem. Eng. Sci.* **1981**, *36*, 993−100.
(24) Watkins, J. J.; Blackburn, J. M.; McCarthy, T. J. *Chem. Mater.* **1999**, *11*, 213−215.
(25) Blackburn, J. M.; Long, D. P.; Watkins, J. J. *Chem. Mater.* **2000**, *12*, 2625−2631.
(26) Long, D. P.; Blackburn, J. M.; Watkins, J. J. *Adv. Mater.* **2000**, *12* (12), 913−915.
(27) Fernandes, N. E.; Fisher, S. M.; Poshusta, J. C.; Vlachos, D. G.; Tsapatsis, M.; Watkins, J. J. *Chem. Mater.* **2001**, *13*, 2023−2031.
(28) Blackburn, J. M.; Long, D. P.; Cabanas, A.; Watkins, J. J. *Science* **2001**, *294*, 141−145.
(29) Cabañas, A.; Shan, X.; Watkins, J. J. *Chem. Mater.* **2003**, *15*, 2910−2916.
(30) Hunde, E.; Watkins, J. J. *Chem. Mater.* **2004**, *16* (3), 498−503.
(31) Kondoh, E.; Kato, H. *Microelectron. Eng.* **2002**, *64*, 495−499.

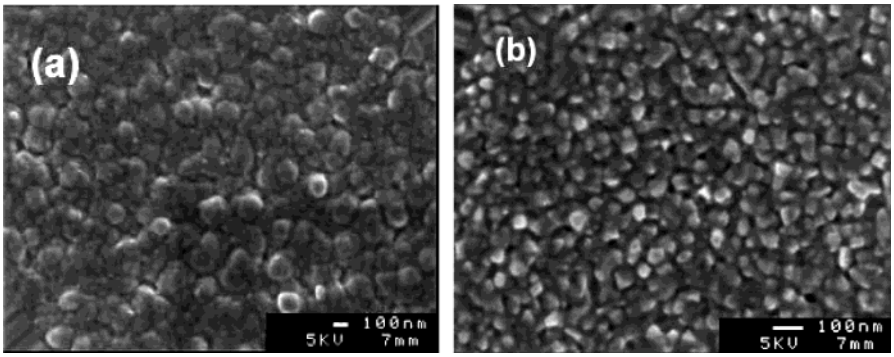

Figure 1. SEM micrograph of a gold film deposited on a Pd-seeded polyimide film (a) and a Ni foil (b) by H_2-assisted reduction of (acac)Au$(CH_3)_2$ in CO_2 solution at 60 °C and 138 bar.

Table 1. Summary of H_2-Assisted Gold Deposition Experiments Performed at 60 °C and 140 Bar CO_2 Using a Hot-Wall Reactor

exp.	substrate[a]	wt. % precursor in CO_2	film thickness (nm)	grain size (SEM) (nm)
1	nickel foil	0.37	90	40−60
2	Ni/Pd/Kapton	0.30	195	20−80
3	Ni/Pd/Kapton	0.67	325	40−80
4	palladium foil	0.34	180	
5	Pd/Kapton	0.43	360	50−200
6	Pd/etched-silicon	0.36	170	50−110
7	Pd/etched-silicon	0.73	120	60−80
8	Pt/Kapton	0.46	105	

[a] Ni/Pd/Pt films or seed layers deposited via CFD at 140 bar and 60 °C except those marked foil.

Table 2. Summary of H_2-Assisted Gold Deposition Experiments Performed at 125 °C

exp.[a]	substrate	wt. % precursor in CO_2	film thickness (nm)	grain size (SEM) (nm)
9	SiO_2	0.10	200	100
10	TiN	0.10	400	75−100
11	SiO_2/etched-silicon trenches	0.08	200	
12	SiO_2/etched-silicon vias	0.24	100	

[a] Experiments 9−11 were conducted using a cold-wall reactor at 150 bar CO_2. Experiment 12 was conducted using a hot-wall reactor at 209 bar CO_2. Deposition time in all cases was 4 h.

The gold deposits were analyzed by X-ray photoelectron spectroscopy (XPS), field-emission scanning electron microscopy (FESEM), and X-ray diffraction (XRD). XPS was carried out using a Quantum 2000 spectrometer (Physical Electronics) with an Al Kα mono source of 1486.6 eV. Atmospheric contaminants were removed from the sample by Ar^+ sputtering (3 keV). FESEM) was carried out on a JEOL JSM 6320 FXV field emission SEM. Cross-sectional SEM of Au films on silicon wafers was conducted after scoring the wafer and fracturing it by hand. X-ray diffraction (XRD) was conducted using a Phillips X'Pert PW 3040 with Cu Kα radiation. In selected cases, the thickness of the film was confirmed using a Dektak^3 profilometer (Veeco Instruments, Inc.).

Organic byproducts contained in the CO_2 effluent were examined by nuclear magnetic resonance spectroscopy (NMR) to determine possible reduction pathways. Proton NMR was performed on Bruker instruments operating at 200 MHz, and ^{2}D NMR was obtained on a Bruker 500 MHz instrument.

Results and Discussion

(acac)Au$(CH_3)_2$ was chosen as precursor for this study because of its solubility in CO_2 and its documented reduction pathways in the literature.[11] It also contains a nonfluorinated ligand system, which is preferable to fluorinated species from an emissions standpoint. Representative deposition conditions and results are summarized in Tables 1 and 2.

At 60 °C, gold metallization was found to be selective for metal surfaces, particularly those of the nickel group versus the native oxide of silicon, glass, or polyimide. Deposition on nongrowth surfaces at this temperature was achieved by depositing a seed layer of an active metal such as Pd, Pt or Ni from carbon dioxide solution prior to gold deposition. Pd and Pt seeds were deposited at 60 °C with the appropriate precursors using techniques described previously. [24,25] Ni seed layers were prepared by co-reduction of [$(Cp)_2$Ni] and [CpPd(π^3-C_4H_7)].[28]

At 60 °C, seed layers of Ni or Pd prepared in CO_2 were found to quantitatively reduce (acac)Au$(CH_3)_2$, yielding bright, reflective, and adherent gold films. On SiO_2 or SiO_2 surfaces seeded with metal clusters, the adhesion of gold was not as good and the deposited film could be removed after a single application of a pressure sensitive adhesive. Cross-sectional SEM analysis of gold films deposited at 60 °C on Pd-seeded Kapton indicated that the films were 300−400 nm thick. Gold films deposited on Ni-seeded polyimide were likewise up to 400 nm thick, bright, reflective, and adherent. An SEM image of the film surface indicates dense surface coverage and does not reveal obvious defects (Figure 1a). Hydrogen reduction yields pure metal films as determined by XPS.[26]

We also carried out gold deposition experiments on Ni and Pd foils. The experiments yielded adherent, but comparatively thinner, films at equivalent deposition conditions. This is probably due to the increased surface area of Ni films deposited by the CFD method, in comparison to the relatively smooth surface of Ni foil. The presence of impurities in the commercial metal foils, however, cannot be ruled out. An SEM image of a gold film deposited on a nickel foil at 60 °C and 138 bar is shown in Figure 1b. The image reveals well-defined Au crystals between 40 and 60 nm in size.

By increasing the temperature to 125 °C, highly reflective, 100−400-nm-thick gold films were readily deposited directly on the native oxide of Si and TiN films, from 0.10 wt % solutions of (acac)Au$(CH_3)_2$ in $scCO_2$ (Table 2). Reactions were performed in both cold- and hot-wall reactors. Figure 2 shows a SEM of a gold film deposited at 125 °C and 150 bar on SiO_2. A similar structure was observed for films grown on TiN. In both

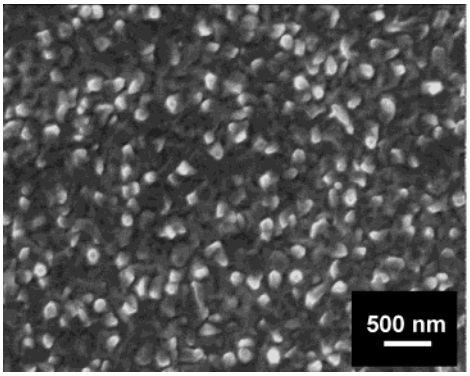

Figure 2. SEM micrograph of a gold film deposited on a bare silicon wafer by H_2-assisted reduction of (acac)Au$(CH_3)_2$ in CO_2 solution at 125 °C and 150 bar.

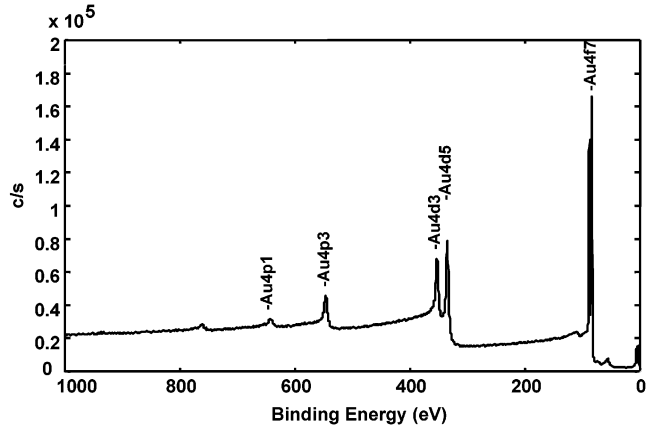

Figure 3. XPS spectrum of a gold film deposited onto a bare Si wafer by H_2-assisted reduction of (acac)Au$(CH_3)_2$ in CO_2 solution at 125 °C and 150 bar.

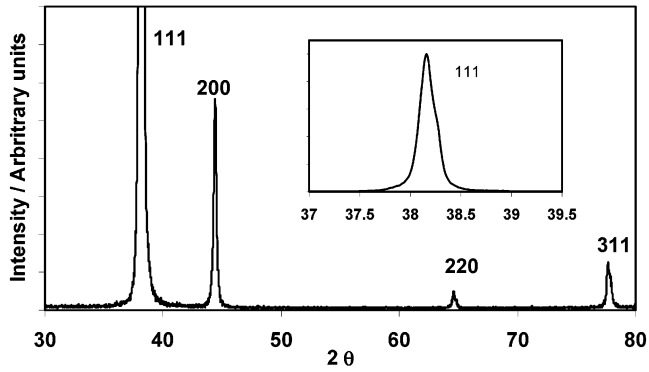

Figure 4. XRD pattern of a gold film deposited on a bare Si wafer by H_2-assisted reduction of (acac)Au$(CH_3)_2$ in CO_2 solution at 125 °C and 150 bar.

cases, the primary grain size was larger than that of films deposited at 60 °C, between 100 and 150 nm. At 125 °C, films were comparatively thicker on TiN than on SiO_2.

Figure 3 shows an XPS survey analysis (45 degree takeoff angle) of a Au film deposited onto a bare silicon wafer at 125 °C and 150 bar. After Ar^+ sputtering to remove atmospheric contaminants, the levels of carbon and oxygen are below the instrument detection limit. XRD analysis of the same film is shown in Figure 4.

Experiments using patterned Si substrates containing narrow, high aspect ratio features indicated that at both 60 °C on Pd-seeded wafers and at 125 °C on unseeded wafers, gold deposition was conformal. Figure 5 shows SEM images of a gold film deposited onto a bare Si wafer at 125 °C and 150 bar by the H_2-assisted reduction of a 0.08 wt. % solution of (acac)Au$(CH_3)_2$ in $scCO_2$. The deposition was carried out in a cold-wall reactor. Step coverage is excellent as evidenced by void-free trench filling in features less than 100 nm wide by 1 μm deep. Figure 5b is an SEM image of a gold film that has delaminated from a Si substrate containing 200-nm-wide features during fracture of the sample in preparation for imaging, indicating that the film is both continuous and conformal. Adhesion of the gold films deposited on Si substrates at 125 °C was poor.

The exceptional step coverage exhibited by CFD enables a straightforward approach to the fabrication of continuous arrays of high aspect ratio nanostructures (Scheme 1). The procedure involves the H_2-assisted

Scheme 1

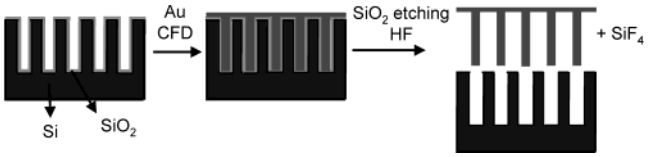

deposition of gold on a sacrificial template prepared by back-filling an etched Si wafer with SiO_2. After gold deposition, the wafer was immersed in a dilute HF solution, which selectively etches SiO_2 and releases the gold film. The film was mounted on an aluminum stub and studied by SEM (Figure 6). The images show self-supporting arrays of regularly spaced, 200-nm-wide gold posts. Although the posts shown in the figure are solid, hollow posts can be prepared by adjusting the thickness of the deposited film.

A similar procedure can likely be employed to produce nanostructures of other metals such as Ni or Cu that exhibit exceptional step coverage during deposition from CO_2.[28]

Reduction Mechanism. The high purity of the deposited films suggests that the ligand byproducts do not fragment. ^{1}H NMR was used to verify this point and to asses the mechanism for the H_2-assisted reduction of (acac)Au$(CH_3)_2$ in $scCO_2$ at the temperature used. Reaction byproducts from deposition experiments were collected for analysis in cold $CDCl_3$. ^{1}H NMR spectrum of (acac)Au$(CH_3)_2$ consists of a single resonance for the two equivalent methyl groups bound directly to the gold-(III) center(1.15 ppm, 6H), a singlet for the equivalent methyl groups of the acac ligand (2.02 ppm, 6H), and a singlet for the lone C−H acac proton (5.34 ppm, 1H).[32] No evidence of the precursor was detected in the analysis of the CO_2 effluent stream following H_2-assisted gold deposition on a Ni-seeded polyimide film at 60 °C and 138 after 24 h. Rather, the appearance of those characteristic of 2,4-pentanedione and ethane indicates that the reaction at these conditions is quantitative and suggests that ligand fragmentation does not occur. (Figure 7).

The single resonances at 2.06 ppm (CH_3), 2.26 ppm (CH_3), 3.60 ppm (CH_2), and 5.51 ppm (CH) are characteristic of 2,4-pentanedione (A) in equilibrium with its

(32) Komiya, S.; Kochi, J. K. *J. Am. Chem. Soc.* **1977**, *99*, 3695−3704.

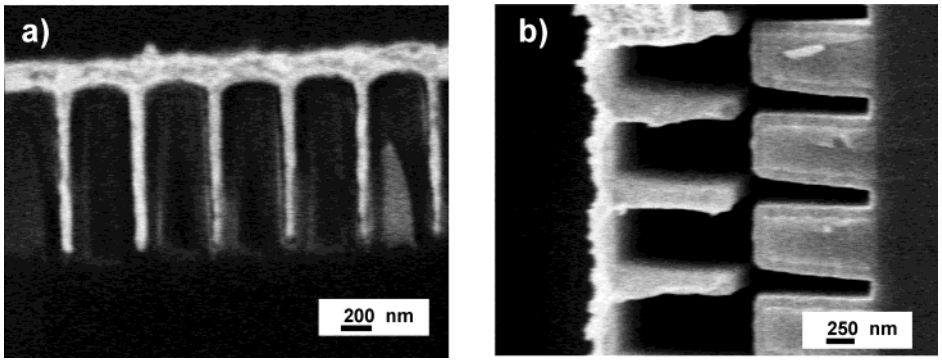

Figure 5. SEM micrographs of gold films deposited onto etched silicon wafers by the H_2-assisted reduction of 0.08 wt % (acac)-$Au(CH_3)_2$ solutions in $scCO_2$ at 125 °C and 150 bar.

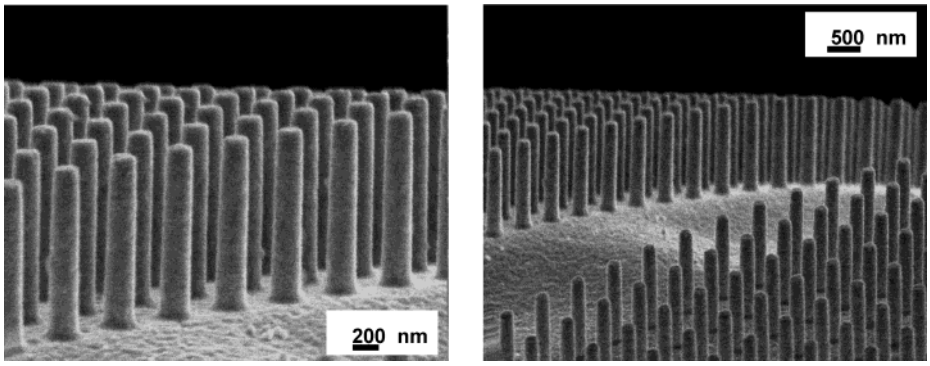

Figure 6. SEM micrograph of self-supporting gold arrays obtained by H_2-assisted reduction of a 0.24 wt % (acac)$Au(CH_3)_2$ solution in $scCO_2$ at 125 °C and 209 bar using a hot-wall reactor.

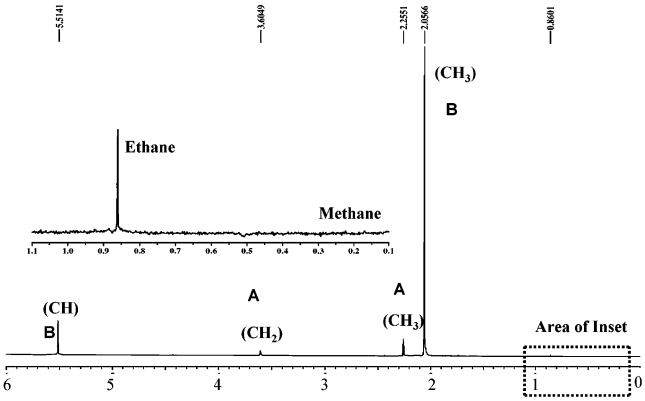

Figure 7. ^1H NMR spectrum of the CO_2 effluent stream of the H_2-assisted reduction of (acac)$Au(CH_3)_2$ in $scCO_2$ on a Ni-seeded polyimide film at 60 °C and 138 bar. Both 2,4-pentadione (A) and its corresponding enolate structure (B) are evident in the spectrum.

corresponding enolate structure (B). The single resonance at 0.860 ppm corresponds to ethane dissolved in $CDCl_3$ produced by the reductive elimination of the methyl groups from the gold complex. The presence of methane (0.227 ppm) was never observed in the ^1H NMR analysis from deposition of gold under any reaction conditions. The formation of ethane from the reductive coupling of the σ-bound methyl groups of the gold complex rather than elimination leading to methane, has been previously observed during CVD using this precursor.[11,33]

^1H NMR analysis of byproducts of the reduction of (acac)$Au(CH_3)_2$ on Ni- and Pd-seeded films on polyimide at 60 °C revealed that reaction on these substrates is generally complete within 4−6 h. Analysis of byproducts of the deposition at 125 °C on a SiO_2 wafer showed that reaction is complete within 4 h. At 125 °C, ^1H NMR spectra again revealed resonance characteristics of ethane and 2,4-pentanedione in equilibrium with its enolate without other major decomposition products.

^1H NMR was also used to probe the nature of strictly thermal decomposition of (acac)$Au(CH_3)_2$ under the conditions used for gold deposition. A Ni film deposited on polyimide was used as the active surface. The substrate was exposed to a 0.7 wt. % solution of (acac)-$Au(CH_3)_2$ in CO_2 at 60 °C and 138 bar for 22 h without the addition of H_2. Gold deposition was not observed and ^1H NMR analysis of the solution confirmed that no thermal decomposition had taken place. The spectrum contained the only characteristic resonance of (acac)-$Au(CH_3)_2$ in $CDCl_3$. The addition of hydrogen is required to initiate the reduction of the gold precursor.

To determine conclusively the participation of hydrogen in the deposition process, deuterium gas (D_2) was used to initiate (acac)$Au(CH_3)_2$ reduction and the effluent stream was analyzed by ^2D NMR. A Ni film deposited on polyimide by CFD was used as the substrate. Au was deposited by reduction of a 0.7 wt. % solution of (acac)$Au(CH_3)_2$ in CO_2 with excess deuterium at 60 °C and 138 bar for 22 h. ^2D NMR spectrum of the reaction byproducts (Figure 8) was referenced to the natural deuterons in the $CHCl_3$ at 7.27 ppm, making the spectrum directly comparable to its proton analogue. The deuterium spectrum shows a major resonance at 5.57 ppm, which corresponds to those deuterons which added into the CH group of the acac ligand and reside on the enolate resonance structure of the deuterated 2,4-

(33) Anderson, G. K. *Adv. Organomet. Chem.* **1982**, *20*, 39.

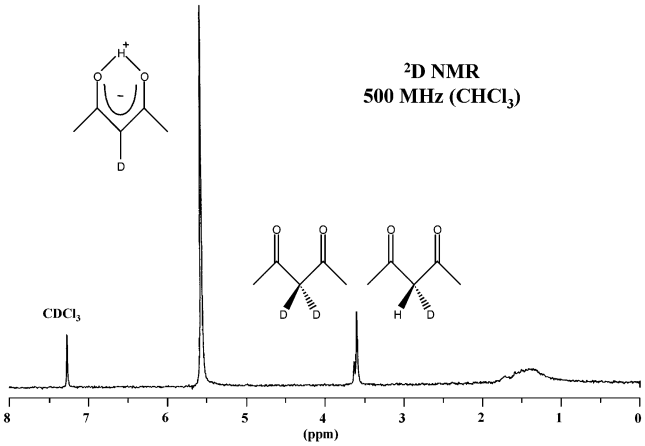

Figure 8. ^{2}D NMR spectrum of CO_2 effluent stream of the D_2-assisted reduction of (acac)Au(CH_3)$_2$ in scCO_2 on nickel-seeded Kapton film at 60 °C and ca 138 bar.

pentanedione [$(CH_3CO)_2C-D]^-$. Two additional singlets were observable at 3.63 and 3.60 ppm and are due to the deuterated β-diketonates [$(CH_3CO)_2CH-D$] and [$(CH_3CO)_2C-D_2$] that form during exchange of protons and deuterons while the β-diketonate exists in its enolate structure. No evidence for the formation of CH_3-D was found during the ^{2}D NMR analysis. Deuterium adds to only the acac ligand of the gold precursor but not to the σ-bound methyl groups directly on the gold center, which undergo homolysis to form ethane. The deuterated 2,4-pentanedione, [$(CH_3CO)_2CH-D$], which is the expected initial reduction product, is also shown by ^{2}D NMR to be exchanging its protons and deuterons to yield [$(CH_3CO)_2C-D_2$].

Conclusions

High-purity gold films were deposited by the H_2-assisted reduction of (acac)Au(CH_3)$_2$ in scCO_2. At 60 °C, deposition was selective for metal surfaces or catalytic seed layers over nongrowth surfaces such as polymers and SiO_2. At 125 °C, gold deposited readily on all surfaces studied, including the native oxide of Si wafers and TiN. The depositions were conformal in all cases. Complete trench filling was demonstrated in etched silicon wafers for the smallest features measuring 0.1 μm wide by 1.0 μm deep. Conformal deposition of gold onto etched silicon wafers backfilled with SiO_2 followed by selective etching of the silicon oxide layer released the gold layer and provided a straightforward route to the fabrication of continuous gold nanostructures.

Acknowledgment. We acknowledge funding from the National Science Foundation (CTS-9734177), the David and Lucile Packard Foundation, and Novellus Systems. Facilities supported by the Materials Research Science and Engineering Center at the University of Massachusetts were used for film characterization. We thank Scott Fisher and Xiaoying Shan for assistance with SEM and XPS characterization of some of the films.

CM034739U